Electronic Supplementary Material (ESI) for Journal of Materials Chemistry A.

Supporting online Materials for

Highly efficient bifunctional catalytic activity of bismuth rhodium oxide pyrochlore through tuning the covalent character for rechargeable aqueous Na-air batteries

*Myeongjin Kim, Hyun Ju and Jooheon Kim**

School of Chemical Engineering & Materials Science, Chung-Ang University, 211 Heukseok-dong, Dongjak-gu, Seoul 156-756, Republic of Korea

*Corresponding author: Jooheon Kim, Tel:+82-2-820-5763; Fax:+82-2-812-3495; E-mail address: jooheonkim@cau.ac.kr (J. Kim)

Materials and methods

Preparation of phosphate ion functionalized $Bi_2Rh_2O_{6.8}$. The buffer solution was made with a mixture of 1 M ammonia solution, 3.42×10^{-2} mol anhydrous ethylenediaminetetraacetic acid and 1.5 mL nitric acid at a solution pH of 7. To prepare the $Bi_2Rh_2O_{6.8}$, 0.3173 g of bismuth (III) acetate, 0.2374 g of rhodium (III) nitrate solution and 10 g anhydrous citric acid were dissolved and stirred with the buffer solution for 24 h at 150 °C. The gelled solution was dried in an oven at 200 °C for 12 h. The prepared dried powder was crystallized at 1350 °C for 8 h to produce single crystalline $Bi_2Rh_2O_{6.8}$ nanoparticles. In order to functionalize the phosphate ion, the $Bi_2Rh_2O_{6.8}$ nanoparticles were suspended in a 0.5 M ammonium dihydrogen phosphate solution at 120 °C for 36 h. After the treatment, the resulting particles were rinsed with deionized water, filtered several times and vacuum-dried at 80 °C for 12 h.

Electrochemical characterization. The OER/ORR activities were measured using a rotating disk electrode (RDE) and a three-electrode electrochemical cell. A Pt wire, Ag/AgCl, and glassy carbon rotating disk electrode were used as a counter, reference and working electrode. The electrolyte used in OER/ORR was 0.1 m KOH solution. Pure oxygen gas (99.9%) was purged for 30 min before RDE experiment to make the electrolyte saturated with oxygen. The catalyst (7.5 mg) was mixed with deionized water (0.1 mL), ethanol (0.86 mL), and 5 wt% Nafion (0.038 mL, 5 wt% in isopropanol). The resulting slurry was ultra-sonicated for 30 min to generate a catalyst ink. The ink (10.0 μL) was pipetted onto the 0.2475 cm^2 glassy carbon electrode. Pt on Vulcan carbon black (Pt/C, JM) and 20 wt% Ir on Vulcan (Ir/C, Premetek) were measured for comparison. The catalyst ink was prepared as follows. The Pt/C (or Ir/C) catalyst (5 mg) was mixed with deionized water (0.1 mL), ethanol (1.06 mL), and 5 wt% Nafion (0.04 mL, in isopropanol). The resulting slurry was ultrasonicated for 30 min to generate a catalyst ink. The ink (6.0 μL) was pipetted onto the 0.2475 cm^2 glassy carbon electrode. All potentials are reported versus the RHE, and for conversion of the obtained potential (vs Ag/AgCl) to RHE, the following equation:

$$E_{RHE} = E_{Ag/AgCl} + 0.0592\ pH + E_{Ag/AgCl}^0 \tag{1}$$

Where, $E_{Ag/AgCl}^0$ (in 1 M KCl) = +0.235 V, pH = 12.9 for 0.1 M KOH. Koutecky-Levich (K-L) plots were evaluated at various potentials. The slope of their best linear fit lines was used to calculate the number electrons transferred (n) on the basis of the following:

$$\frac{1}{J}=\frac{1}{J_L}+\frac{1}{J_K}=\frac{1}{B\omega^{1/2}}+\frac{1}{J_K} \tag{2}$$

where, J is the measured disk current density; J_K and J_L are the kinetic and diffusion limiting current densities, respectively; and ω is the electrode rotation speed. B is the so-called "B-factor", which is given by the following equation:

$$B = 0.62nFC_oD_o^{2/3}\nu^{-1/6} \tag{3}$$

where n is the apparent number of electrons transferred in the reaction, F is the Faraday constant (96485 C mol^{-1}), D_o is the diffusion coefficient of O_2 in 0.1 M KOH (1.9×10^{-5} cm^2 s^{-1}), ν and C_o are the kinetic viscosity of the solution (0.01 cm^2 s^{-1}) and the concentration of O_2 dissolved in 0.1 M KOH (1.2×10^{-6} mol cm^{-3}). The constant 0.62 is adopted when the rotation speed is expressed in rad.

Anode and electrolyte preparatoin. A Na metal (99.9%) was purchased from Sigma-Aldrich, and was attached to the surface of Ni mesh for use as the anode. An organic nonaqueous liquid electrolyte, 1 M $NaCF_3SO_3$ in tetraethylene glycol dimethyl ether (TEGDME) and an aqueous liquid electrolyte of 0.1 M NaOH aqueous solution were purchased from Sigma-Aldrich. A Na super ionic conducting (NASICON) membrane, $Na_3Zr_2Si_2PO_{12}$, ceramic plate was used as the solid electrolyte. $Na_3Zr_2Si_2PO_{12}$ was prepared by a solid-state reaction method reported elsewhere.[1,2]

Air cathode preparatoin. The air cathode included a catalyst layer and a gas diffusion layer. Teflon-treated carbon paper (Fuel Cell Store) was used as the gas diffusion layer. Catalyst ink solutions were prepared by mixing the P-$Bi_2Rh_2O_{6.8}$ (90 wt%) with polyvinylidene fluoride (10 wt%) as a binder and *N*-methyl-2-pyrrolidone as a solvent. The catalyst ink solution was sprayed onto one side of the Teflon-treated carbon paper. The area of the air electrode was 4 cm^2, and the mass loading of the catalyst layer was 2.5 mg cm^{-2}.

Na-air battery assembly and testing. In order to construct the aqueous Na–air cell, initially, the negative electrode was fabricated in a glove box as the pouch cell. The metallic sodium electrode attached with nickel mesh was inserted into the pouch cell, followed by injection of an organic electrolyte. Thereafter, the separator solid electrolyte membrane (NASICON) was introduced and the pouch cell was sealed in the globe box with one side of the solid electrolyte membrane exposed to air and the other side in contact with the organic electrolyte (1 M $NaCF_3SO_3$/TEGDME). The cathode compartment was fabricated by directly dipping the P-$Bi_2Rh_2O_{6.8}$ air electrode in aqueous electrolyte (0.1 M NaOH) and exposing to ambient air. As a control cathode compartment, Pt/C-coated carbon paper, Ir/C-coated carbon paper, and bare carbon paper were also prepared by the same process. The power density was calculated by following equation:

$$P_s = I_s \text{ x } V_{ad} \tag{4}$$

where P_s, I_s and V_{ad} are power density, applied current density and average discharge voltage, respectively.

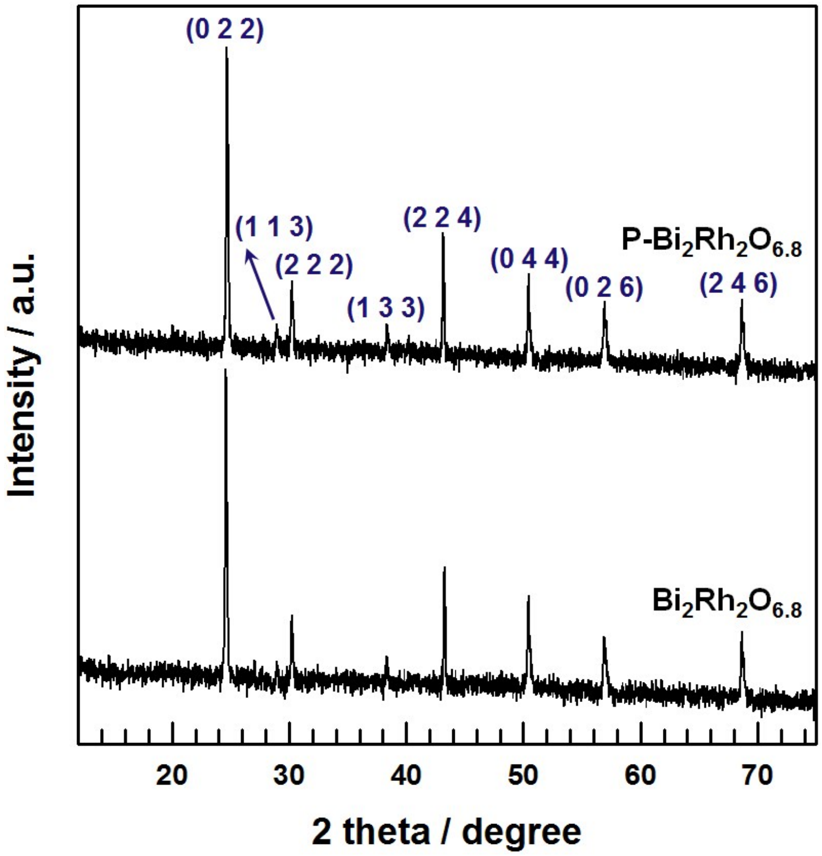

Figure S1. XRD patterns for P-$Bi_2Rh_2O_{6.8}$ and $Bi_2Rh_2O_{6.8}$.

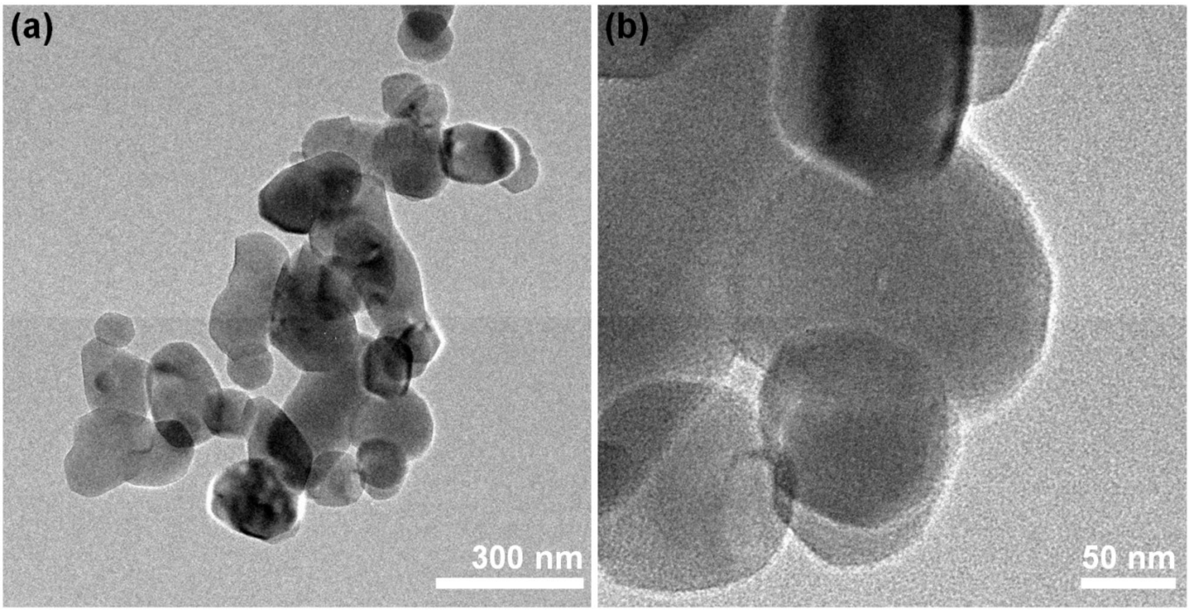

Figure S2. (a) Low magnification of HR-TEM image for P-$Bi_2Rh_2O_{6.8}$. (b) High magnification of HR-TEM image for P-$Bi_2Rh_2O_{6.8}$.

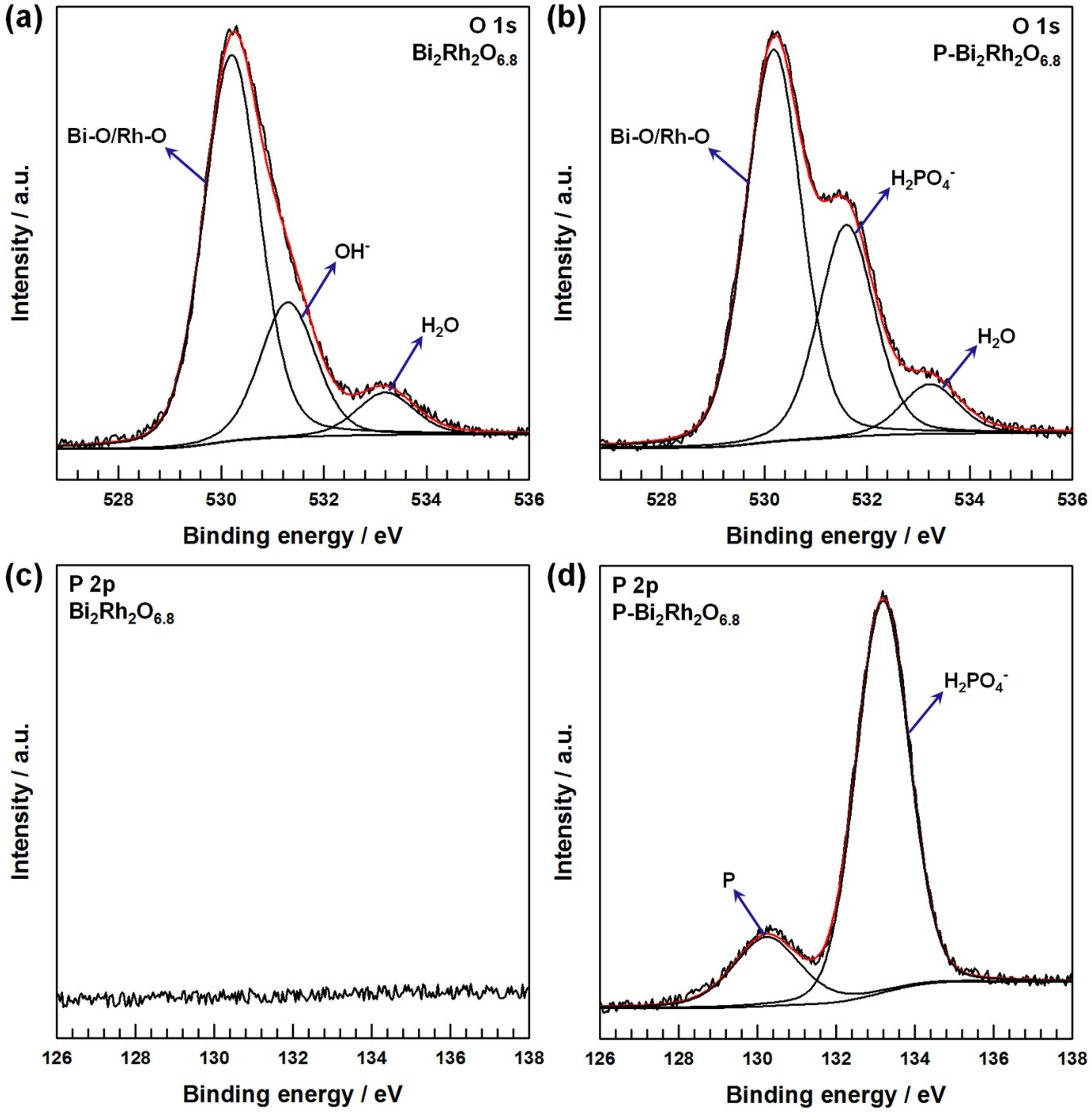

Figure S3. (a) XPS O 1s spectra of $Bi_2Rh_2O_{6.8}$. (b) XPS O 1s spectra of P-$Bi_2Rh_2O_{6.8}$. (c) XPS P 2p spectra of $Bi_2Rh_2O_{6.8}$. (d) XPS P 2p spectra of P-$Bi_2Rh_2O_{6.8}$.

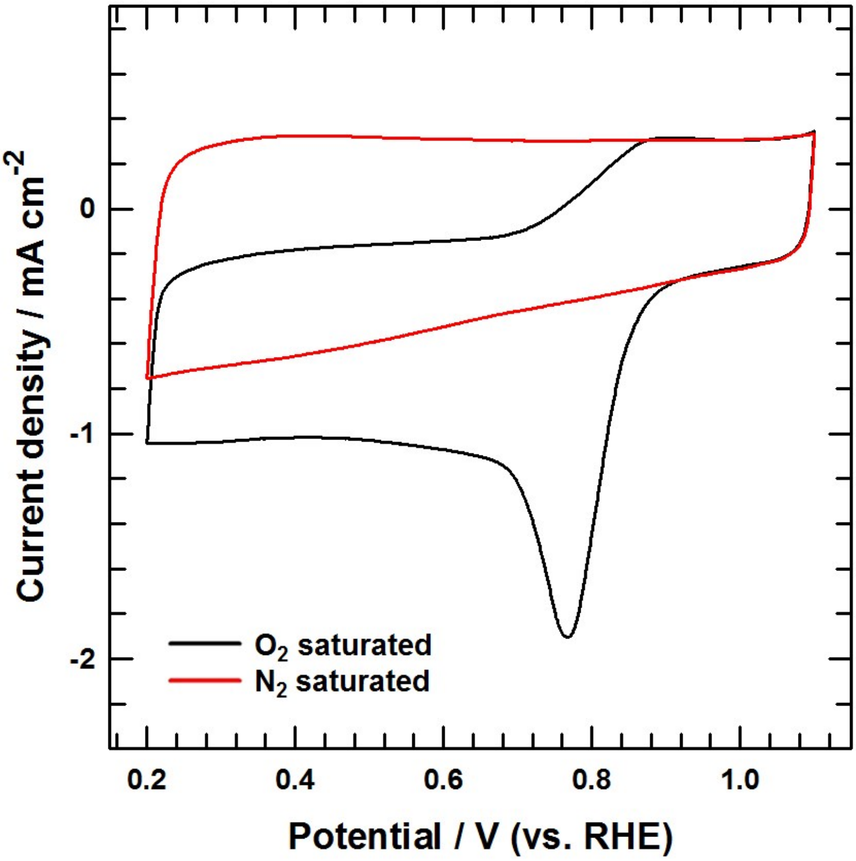

Figure S4. CV curves for $Bi_2Rh_2O_{6.8}$ in N_2 and O_2 saturated 0.1 M KOH solution with a scan rate of 100 mV s^{-1}.

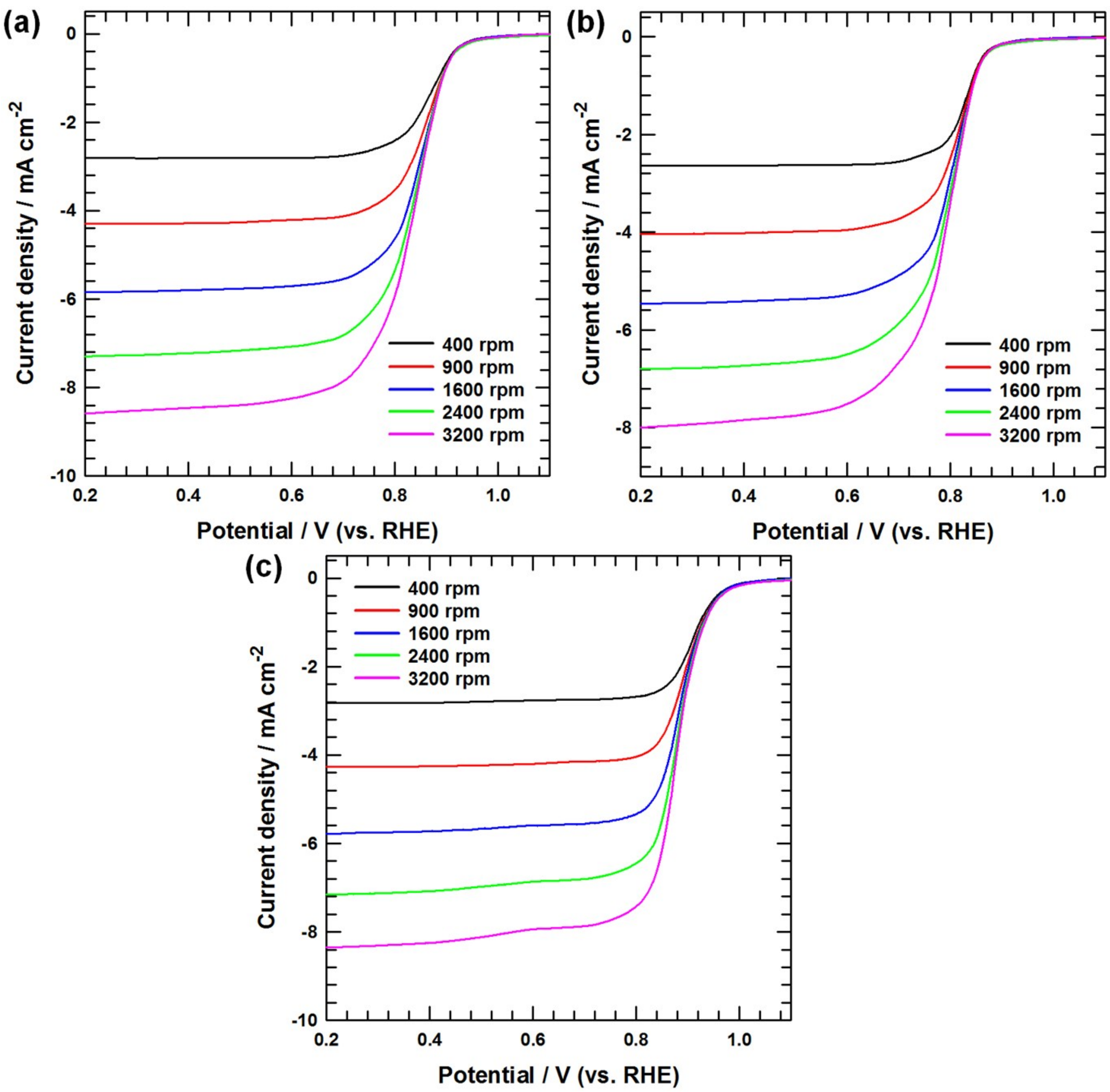

Figure S5. (a) ORR LSV curves for P-$Bi_2Rh_2O_{6.8}$ at different rotating speeds with a scan rate of 10 mV s^{-1}. (b) ORR LSV curves for $Bi_2Rh_2O_{6.8}$ at different rotating speeds with a scan rate of 10 mV s^{-1}. (b) ORR LSV curves for Pt/C at different rotating speeds with a scan rate of 10 mV s^{-1}.

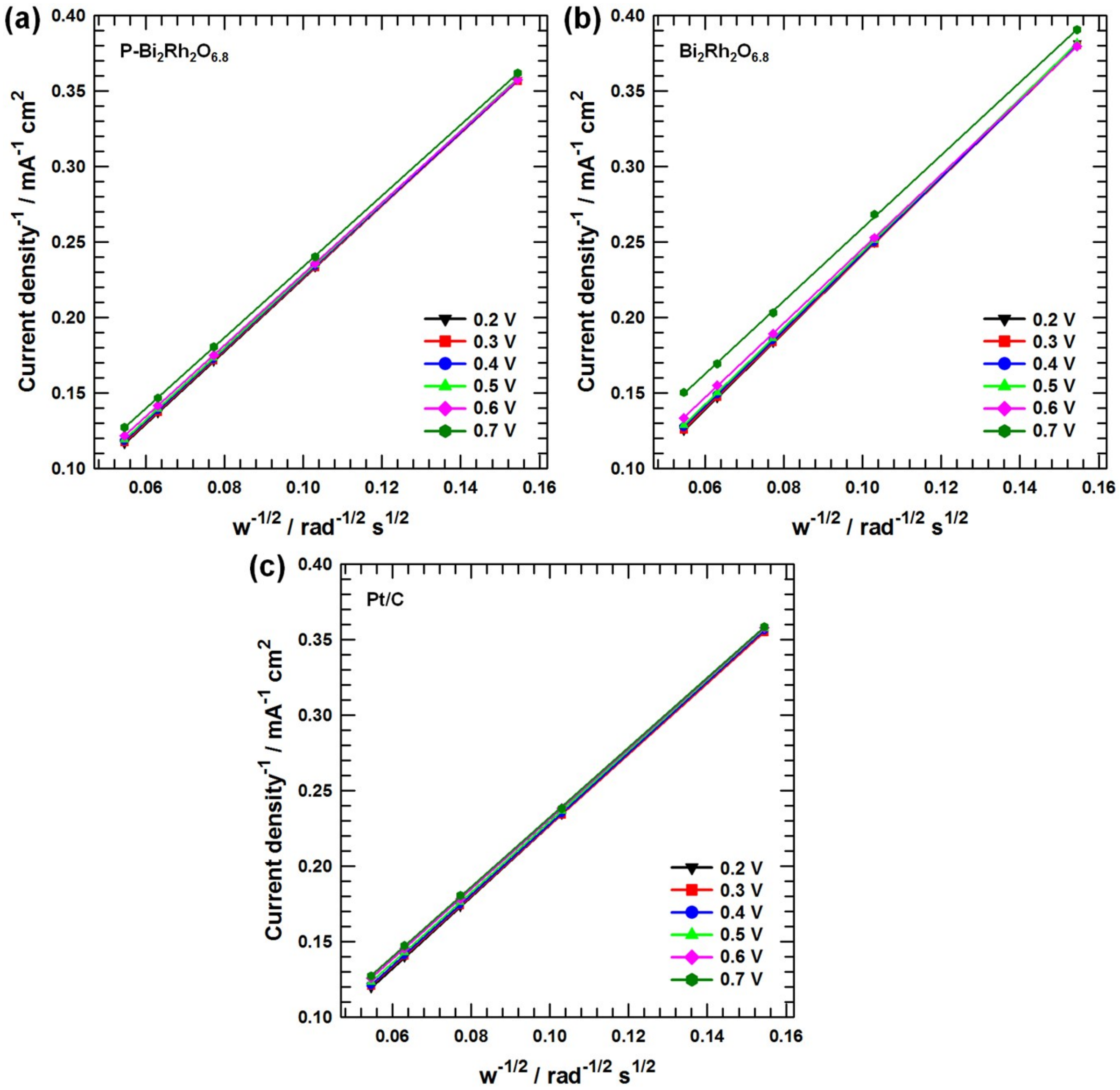

Figure S6. (a) Koutecky-Levich plots derived from the ORR LSV curves of P-Bi$_2$Rh$_2$O$_{6.8}$. (b) Koutecky-Levich plots derived from the ORR LSV curves of Bi$_2$Rh$_2$O$_{6.8}$. (c) Koutecky-Levich plots derived from the ORR LSV curves of Pt/C.

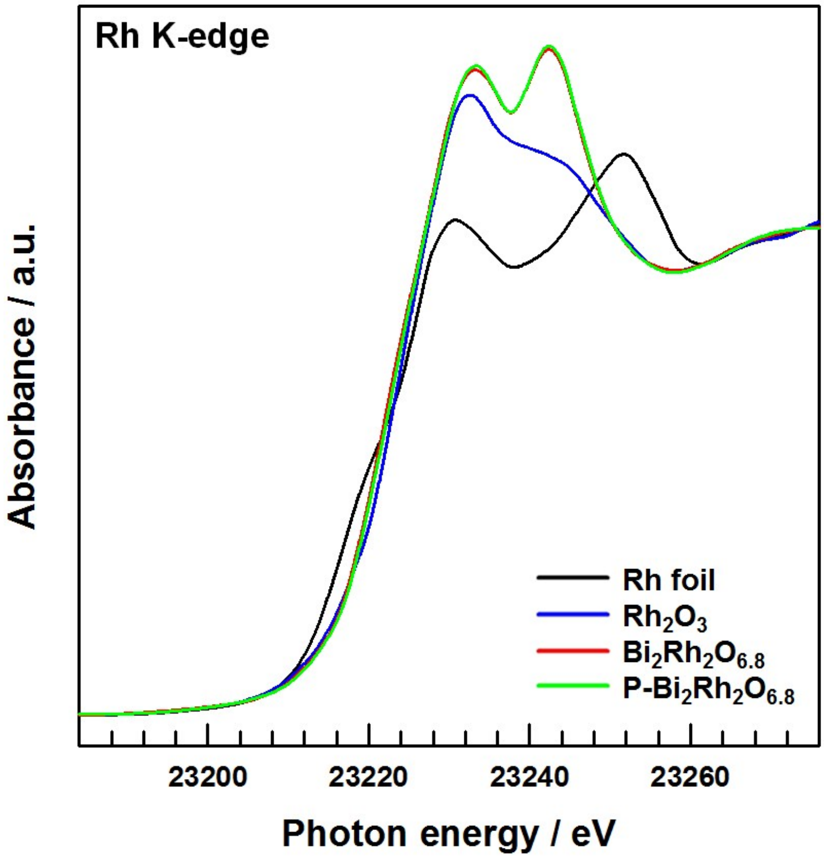

Figure S7. Normalized Rh K-edge XANES spectra of Rh foil, Rh_2O_3, $P-Bi_2Rh_2O_{6.8}$ and $Bi_2Rh_2O_{6.8}$.

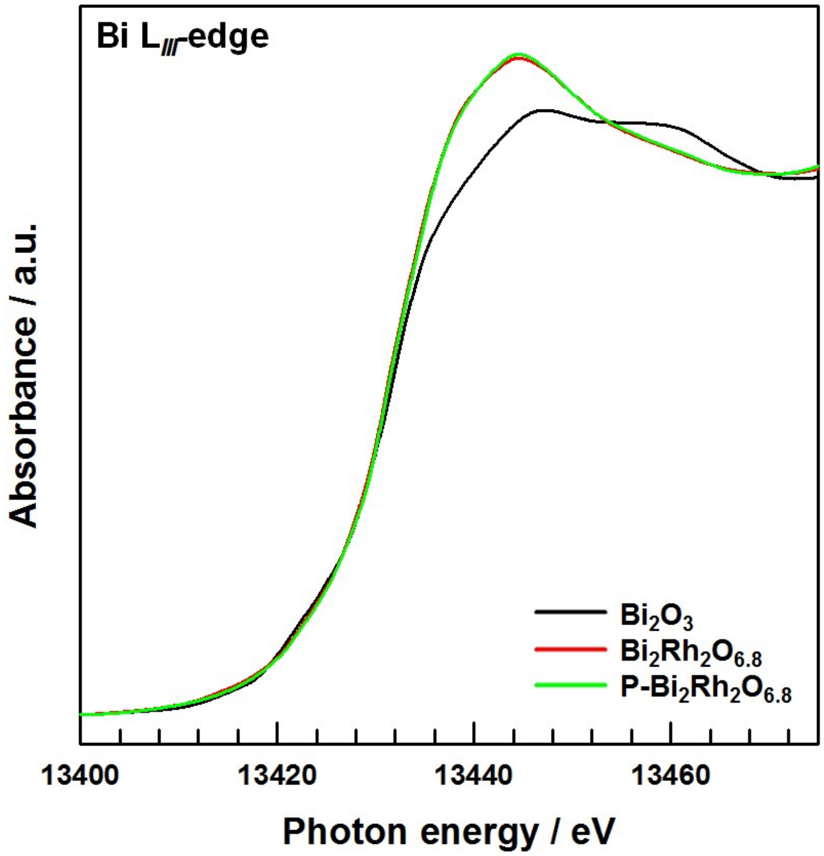

Figure S8. Normalized Bi L_{III}-edge XANES spectra of Bi_2O_3, P-$Bi_2Rh_2O_{6.8}$ and $Bi_2Rh_2O_{6.8}$.

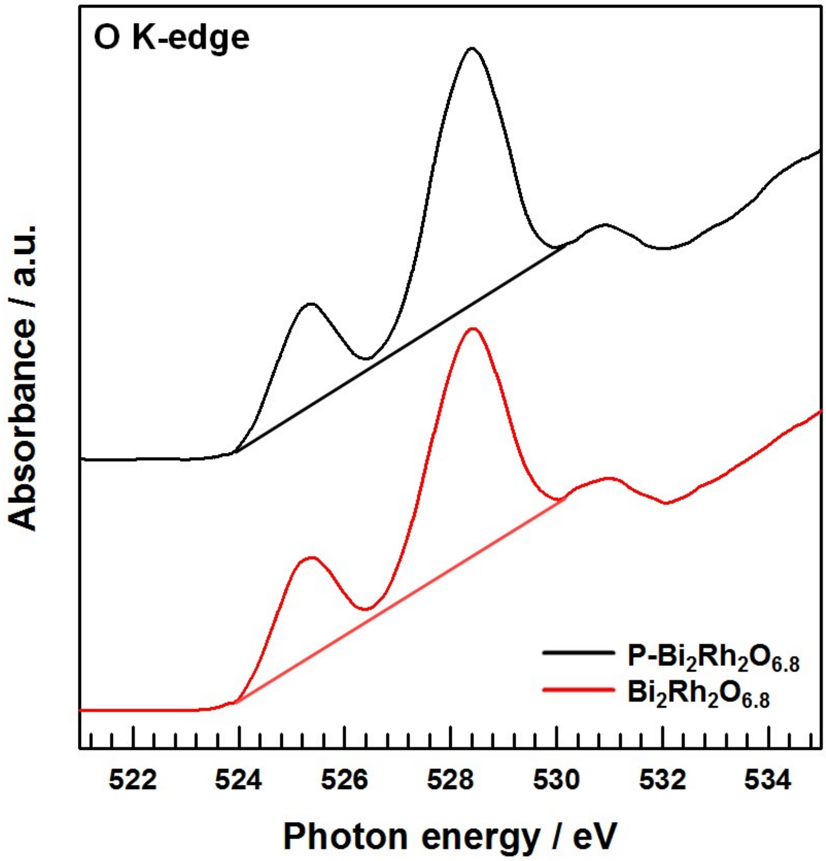

Figure S9. Normalized O K-edge XANES total electron yield mode spectra of the P-$Bi_2Rh_2O_{6.8}$ and $Bi_2Rh_2O_{6.8}$.

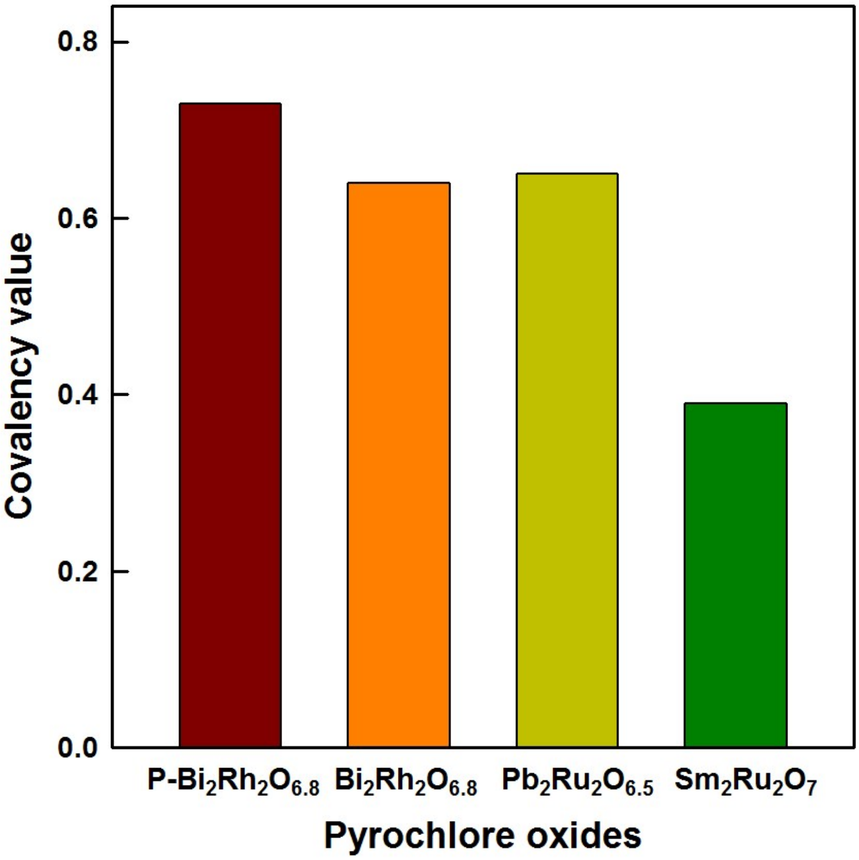

Figure S10. Comparison of covalency value of P-Bi$_2$Rh$_2$O$_{6.8}$, Bi$_2$Rh$_2$O$_{6.8}$, Pb$_2$Ru$_2$O$_{6.5}$ and Sm$_2$Ru$_2$O$_7$.

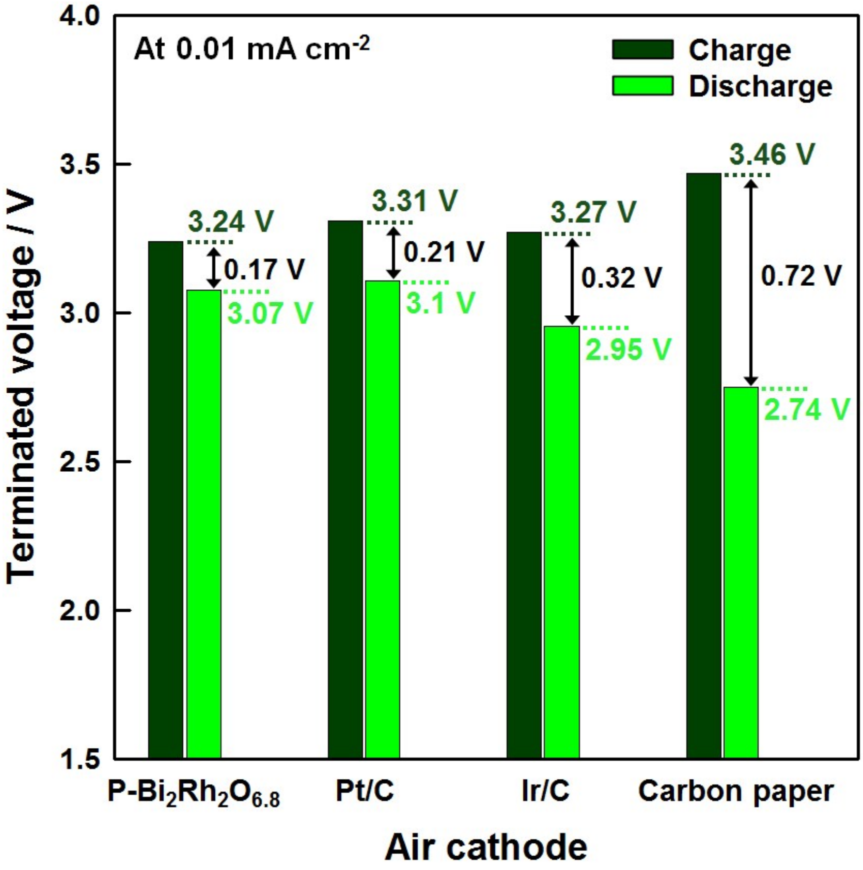

Figure S11. Comparison of the overpotential gap of the P-$Bi_2Rh_2O_{6.8}$, Pt/C, Ir/C and carbon paper.

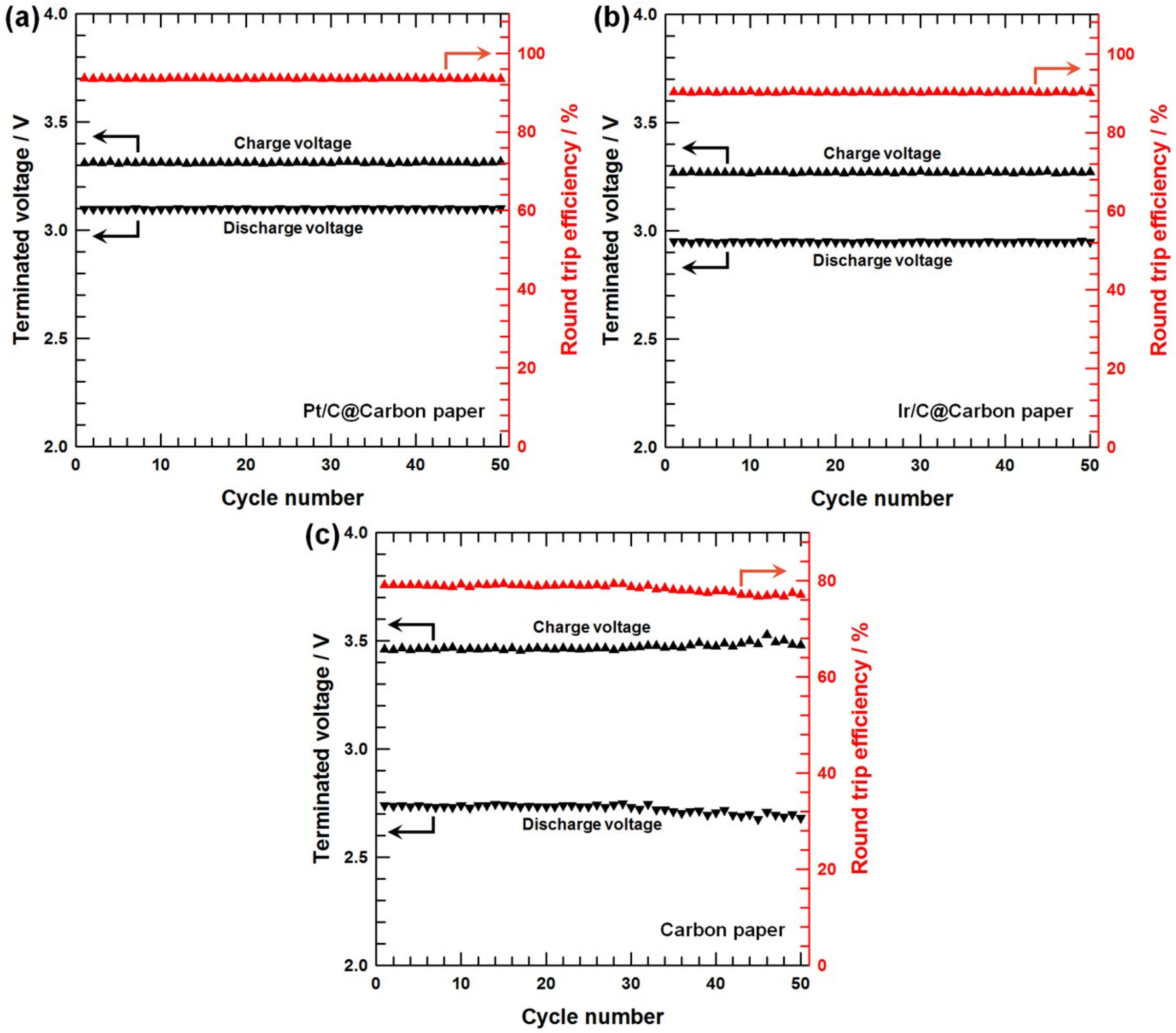

Figure S12. Cycling stability of (a) Pt/C, (b) Ir/C and (c) carbon paper electrode up to 50 cycles with terminated charge and discharge voltage and round trip efficiency.

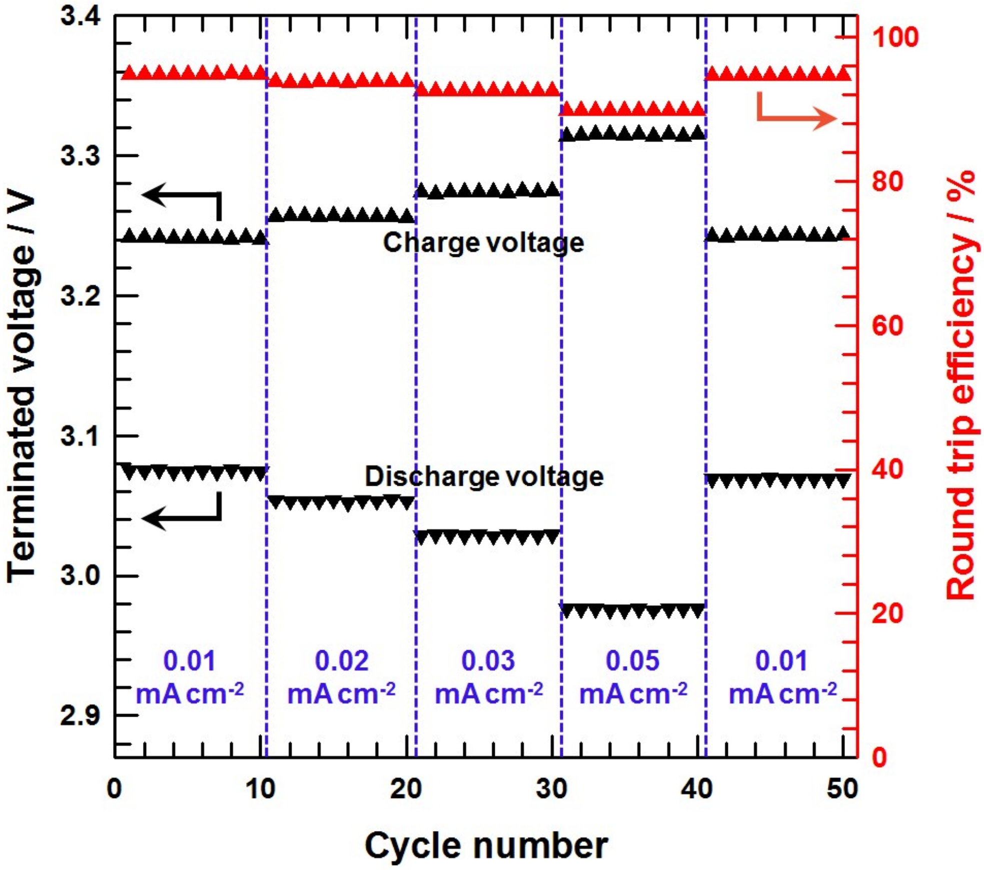

Figure S13. Cycling terminated charge and discharge voltage and round trip efficiency profile of P-$Bi_2Rh_2O_{6.8}$ at different current densities.

Table S1. Comparison of the ORR activity of P-$Bi_2Rh_2O_{6.8}$ with other electrocatalysts previously reported.

Catalyst	Electrolyte	E_{ORR} [at -3 mA cm^{-2}]	Ref
Mn oxide	0.1 M KOH	0.73V	3
PCN-CFP	0.1 M KOH	0.67V	4
Ni_3Fe/N-C sheets	0.1 M KOH	0.78V	5
$NiCo_2O_4$/G	0.1 M KOH	0.56V	6
N, S-CN	0.1 M KOH	0.77V	7
Co_3O_4/2.7Co_2MnO_4	0.1 M KOH	0.68V	8
Co/N-C-800	0.1 M KOH	0.74V	9
$NiCo_2S_4$@N/S-rGO	0.1 M KOH	0.72V	10
$Bi_2Rh_2O_{6.8}$	0.1 M KOH	0.797V	This work
P-$Bi_2Rh_2O_{6.8}$	0.1 M KOH	0.846V	This work

Table S2. Comparison of oxygen electrode activity of P-$Bi_2Rh_2O_{6.8}$ with other electrocatalysts previously reported, including metal oxide based, perovskite based carbon based, pyrochole oxide based bifunctional electrocatalysts.

Catalyst		$E_{OER, \text{ at 10 mA cm-2}}$ - $E_{ORR, \text{ at -3 mA cm-2}}$	Ref
Metal oxide-based	CoO/N-Graphene	0.76V	11
	MnO_x Film	1.06V	12
	$MnCoO_x$/N-Carbon	0.84V	13
	Co_3O_4/N-Graphene	0.71V	14
	Co_3O_4-Carbon	0.74V	15
	$NiCo_2O_4$/Graphene	0.96V	6
	Mn_xO_y/N-Carbon	0.87V	16
	LT-$Li_{0.5}CoO_2$	1.00V	17
	Co_3O_4/N,S-Carbon	0.79V	18
Perovskite-based	La(BaSr)CoFeO	1.01V	19
	$LaNiO_{3-\delta}$	1.04V	20
	ns$LANiO_3$/N-Carbon	0.97V	21
	$LaNiO_3$/N-CNT	0.95V	22
Carbon-based	N-Graphene/CNT	0.95V	23
	N-Carbon	0.84V	24
	Fe, N-Carbon	0.76V	25
	N-CNT/Graphene	0.91V	26
	P, N-Carbon Fiber	0.96V	4
	GNS/MC	0.72V	27
	Fe-Mc	0.88V	27
	N, S, Fe-Carbon	0.91V	28
Pyrochlore oxide-based	$Pb_2Ru_2O_{6.5}$	0.82V	29

	$Y_2[Ru_{2-x}Y_x]O_{7-y}$	1.03V	30
	$Bi_2Rh_2O_{6.8}$	0.87V	This work
	P-$Bi_2Rh_2O_{6.8}$	0.67V	This work

Table S3. Comparison of electrochemical performance of P-$Bi_2Rh_2O_{6.8}$ with other air electrodes previously reported

Na-air battery	Current density	Round trip Efficiency	Cycles	Power density	Ref
Graphitic nanoshell/mesoporous carbon // Aqueous	N/A	96.2%	10	78.2 mW g^{-1} at 60 mA g^{-1}	27
VGC // Aqueous	4 mA g^{-1}	81%	50	104 mW g^{-1} at 80 mA g^{-1}	31
Porous $CaMnO_3$/C // Non-Aqueous	100 mA g^{-1}	55%	80	N/A	32
MnO_2/rGO/carbon paper // Aqueous	15 mA g^{-1}	81%	20	N/A	33
Pt/C // Aqueous	0.025 mA g^{-1}	84.3%	18	N/A	34
$Co_3(PO_4)_2$ // Aqueous	0.05 mA cm^{-2}	83%	50	N/A	35
P-$Bi_2Rh_2O_{6.8}$ // Aqueous	0.01 mA cm^{-2}	94.9%	50	181.2 mW g^{-1} at 120 mA g^{-1}	This work

Reference

1. H. Kim, J.-S. Park, S. H. Sahgong, S. Park, J.-K. Kim and Y. Kim, *J. Mater. Chem. A*, 2014, **2**, 19584–19588.
2. J.-K. Kim, E. Lee, H. Kim, C. Johnson, J. Cho and Y. Kim, *ChemElectroChem*, 2015, **2**, 328–332.
3. Y. Gorlin and T. F. Jaramillo, *J. Am. Chem. Soc.*, 2010, **132**, 13612-13614.
4. T. Y. Ma, J. Ran, S. Dai, M. Jaroniec and S. Z. Qiao, *Angew. Chem. Int. Edit.*, 2015, **54**, 4646-4650.
5. G. Fu, Z. Cui, Y. Chen, Y. Li, Y. Tang and J. B. Goodenough, *Adv. Energy Mater.*, 2017, **7,** 1601172.
6. D. U. Lee, B. J. Kim and Z. Chen, *J. Mater. Chem. A*, 2013, **1**, 4754-4762.
7. K. Qu, Y. Zheng, S. Dai and S. Z. Qiao, *Nano Energy*, 2016, **19**, 373-381.
8. D. Wang, X. Chen, D. G. Evans and W. Yang, *Nanoscale*, 2013, **5**, 5312-5315.
9. Y. Su, Y. Zhu, H. Jiang, J. Shen, X. Yang, W. Zou, J. Chen and C. Li, *Nanoscale*, 2014, **6**, 15080-15089.
10. Q. Liu, J. Jin and J. Zhang, *ACS Appl. Mater. Interfaces*, 2013, **5**, 5002-5008.
11. S. Mao, Z. Wen, T. Huang, Y. Hou and J. Chen, *Energy Environ. Sci.*, 2014, **7**, 609-616.
12. Y. Gorlin, B. Lassalle-Kaiser, J. D. Benck, S. Gul, S. M. Webb, V. K. Yachandra and J. Yano, T. F. Jaramillo, *J. Am. Chem. Soc.*, 2013, **135**, 8525-8534.
13. A. Zhao, J. Masa, W. Xia, A. Maljusch, M.-G. Willinger, G. Clavel,K. Xie, R. Schlögl, W. Schuhmann and M. Muhler, *J. Am. Chem. Soc.*, 2014, **136**, 7551-7554.
14. Y. Liang, Y. Li, H. Wang, J. Zhou, J. Wang, T. Regier and H. Dai, *Nat. Mater.*, 2011, **10**, 780.
15. T. Ma, S. Dai, M. Jaroniec and S. Z. Qiao, *J. Am. Chem. Soc.*, 2014, **136**, 13925-13931.
16. J. Masa, W. Xia, I. Sinev, A. Zhao, Z. Sun, S. Grützke, P. Weide, M. Muhler and W. Schuhmann, *Angew. Chem. Int. Ed.,* 2014, **53**, 8508-8512.
17. T. Maiyalagan, K. A. Jarvis, S. Therese, P. J. Ferreira and A. Manthiram, *Nat. Commun.,* 2014, **5**, 3949.
18. C. Zhang, M. Antonietti and T. P. Fellinger, *Adv. Funct. Mater.,* 2014, **24**, 7655-7665.
19. J. I. Jung, H. Y. Jeong, J. S. Lee, M. G. Kim and J. Cho, *Angew. Chem. Int. Ed.,* 2014, **126**, 4670-4674.

20. W. Zhou and J. Sunarso, *J. Phys. Chem. Lett.,* 2013, **4**, 2982-2988.

21. W. G. Hardin, D. A. Slanac, X. Wang, S. Dai, K. P. Johnston and K. J. Stevenson, *J. Phys. Chem. Lett.,* 2013, **4**, 1254-1259.

22. Z. Chen, A. Yu, D. Higgins, H. Li, H. Wang and Z. Chen, *Nano Lett.,* 2012, **12**, 1946-1952.

23. Z. Wen, S. Ci, Y. Hou and J. Chen, *Angew. Chem. Int. Ed.,* 2014, **53**, 6496-6500.

24. Y. Zhao, R. Nakamura, K. Kamiya, S. Nakanishi and K. Hashimoto, *Nat.Commun.,* 2013, **4**, 2390.

25. Y. Zhao, K. Kamiya, K. Hashimoto and S. Nakanishi, *J. Phys. Chem. C,* 2015, **119**, 2583-2588.

26. H. W. Park, D. U. Lee, Y. Liu, J. Wu, L. F. Nazar and Z. Chen, *J. Electrochem. Soc.,* 2013, **160**, A2244-A2250.

27. J. Y. Cheon, K. Kim, Y. J. Sa, S. H. Sahgong, Y. Hong, J. Woo,S.-D. Yim, H. Y. Jeong, Y. Kim and S. H. Joo, *Adv. Energy Mater.*, 2016, **6**, 1501794.

28. N. R. Sahraie, J. P. Paraknowitsch, C. Gobel, A. Thomas and P. Strasser, *J. Am. Chem. Soc.,* 2014, **136**, 14486-14497.

29. J. Park, M. Risch, G. Nam, M. Park, T. J. Shin, S. Park, M. G. Kim, Y. Shao-Horn and J. Cho, *Energy Environ. Sci.,* 2017, **10**, 129-136.

30. J. Park, M. Park, G. Nam, M.-G. Kim and J. Cho, *Nano Letters,* 2017, **17**, 3974-3981.

31. Z. Khan, B. Senthilkumar, S. O. Park, S. Park, J. Yang, J. H. Lee, H.-K. Song, Y. Kim, S. K. Kwak and H. Ko, *J. Mater. Chem. A,* 2017, **5**, 2037-2044.

32. Y. Hu, X. Han, Q. Zhao, J. Du, F. Cheng and J. Chen, J. *Mater.Chem. A,* 2015, **3**, 3320–3324.

33. Z. Khan, S. Park, S. M. Hwang, J. Yang, Y. Lee, H.-K. Song, Y. Kim and H. Ko, *NPG Asia Mater.*, 2016, **8**, e294.

34. S. H. Sahgong, S. T. Senthilkumar, K. Kim, S. M. Hwang and Y. Kim, *Electrochem. Commun.*, 2015, **61**, 53–56.

35. B. Senthilkumar, Z. Khan, S. Park, I. Seo, H. Ko and Y. Kim*, J. Power Sources*, 2016, **311**, 29–34.